

centre de recherches nucléaires de Strasbourg

C.R.N.

CRN/PN.76-11
FR760 2104

DETECTION OF NEUTRONS
OF INTERMEDIATE ENERGY USING ^{10}B ,
ENCLOSED IN A COAXIAL Ge(Li) COUNTER

A. HUCK, G. KLOTZ and G. WALTER

Laboratoire de Physique des Rayonnements
et d'Electronique Nucléaire

Institut National
de Physique Nucléaire
et de Physique
des Particules

Université
Louis Pasteur
de Strasbourg

67037 STRASBOURG-CEDEX FRANCE

DETECTION OF NEUTRONS OF INTERMEDIATE ENERGY
USING ^{10}B , ENCLOSED IN A COAXIAL Ge(Li) COUNTER

A. HUCK, G. KLOTZ and G. WALTER

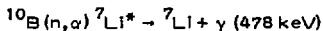
Centre de Recherches Nucléaires
67037 STRASBOURG CEDEX (France)

ABSTRACT

A neutron detector operating in the energy range 1 keV to roughly 1 MeV with a time response that is fast enough to be used in time-of-flight experiments, has been designed and built. The neutron is absorbed in boron-10, placed inside a coaxial Ge(Li) counter. Efficient detection of the 478 keV line from ^7Li , resulting from $^{10}\text{B}(n,\alpha)^7\text{Li}^*$, is realized. At the same time, the measurement of accompanying γ radiations, emitted by the neutron source, can be performed. Examples of results, obtained using (p, n γ) reactions, are given.

I. INTRODUCTION

The detection of low energy neutrons accompanied by high intensity γ rays is not adequately cared for by the existing counters. Boron loaded phosphors and glass scintillators have been used for detection in the 1-1000 keV neutron energy range (1). Discrimination between n and γ activity is not complete in this case. Many detectors (2-6) have been built in which the γ -rays from the reaction



were detected in sodium iodide scintillation spectrometers. For this type of detector, two conditions have to be fulfilled :

- the counting efficiency for γ -rays from $^7\text{Li}^*$ must be high and hence a large solid angle for detection must be obtained by the use of large crystals around the absorbing material ;
- the background has to be minimized using good resolution detectors and electronic windows set to count the total energy peak of the $^7\text{Li}^*$ radiation.

Such a device has been described by RAE and BOWEY (2). In that case, two NaI crystals (4.44 cm diam, x 5.08 cm deep) are placed one on each side of a boron-10 container (7.5 cm diam. and 3.2 cm thick) on opposite ends of a diameter.

The use of a coaxial Ge(Li) counter is well designed to refine this technique. First, the resolution and therefore the signal to background ratio is improved. Furthermore, the boron container can be placed inside the central hole of a coaxial crystal allowing the detection of γ -rays in a close to 4π geometry. The resulting counter has a good efficiency for slow

neutrons and keeps all performances for usual γ detection. It may be of value for different applications as :

- measurement of neutron thresholds with low energy accelerators ;
- time-of-flight measurement of slow neutrons ;
- simultaneous detection of neutrons and gamma rays.

II. DESCRIPTION OF THE COUNTER

The arrangement of the apparatus is shown schematically in Fig. 1. A true coaxial Ge(Li) detector* of 41 cm^3 active volume with a central hole of 15 mm diameter and a total length of 43 mm, was used. In order to make both the absorption and the angle straggling negligible, the entrance window of the cryostat should be as thin as possible. A 0.8 mg/cm^2 aluminized mylar window was used in the system described. A thin-walled (0.75 mm) stainless steel cylinder, 12.2 mm in diameter and 31 mm deep, filled with amorphous boron 10 is located inside the Ge(Li) central hole. A total weight of 2.15 g of enriched (95 %) boron** was compacted in the container. The sealing of the vessel with epoxy was carefully checked, to make sure that no leak could occur at low temperature. The centering and insulating of the cylinder inside the hole was obtained by the mean of a polyethylene sleeve. It appeared useful, in some applications, to decrease the direct gamma efficiency of the counter. An annular lead collimator (5 mm thick), placed in front of the mylar window, was used in these cases.

The fraction of the α -particles from $^{10}\text{B}(n,\alpha)^7\text{Li}$ which populate the excited state of ^7Li is 94 % for thermal energy neutrons (?) and not

*from LASCO, Mundolsheim (France).

**supplied by QUARTZ & SILICE

much different at higher energies. Assuming a variation of $\sigma(n, \alpha)$ proportional to $1/v$ up to 250 keV (8) and fitted by $\sigma = 611/\sqrt{E}$ (E in eV), corresponding for thermal neutrons to $\sigma = 3840$ b (9), one can estimate the fraction of incident neutrons absorbed in the [Ge(Li) + ^{10}B] counter and the detection efficiency for 478 keV gamma rays. We have reported these parameters in table I and for two different values of the boron density corresponding respectively to :

- ^{10}B in powder form, as in our counter (1) ;
- ^{10}B with crystal density (2).

Special techniques, using ^{10}B powder in a matrix of $^{10}\text{B}_4\text{C}$, have been reported (3) and allow to reach 85 per cent of theoretical crystal density. The overall γ efficiency was estimated taking in account photoelectric and Compton processes.

III. EXPERIMENTAL STUDIES

a) $^7\text{Li}(p, n\gamma)^7\text{Be}$

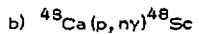
Targets of natural lithium metal were bombarded with the proton beam from the 3 MV Strasbourg Van de Graaff accelerator. In the proton energy range between 1.88 MeV and 2.5 MeV, we have used neutrons from 30 to 800 keV with a monoenergetic neutron group of 120 keV minimum energy at 0° because of center of mass motion. The neutron yield curve, measured with the [Ge(Li) + ^{10}B] counter was recorded with the detector at 0° and the same experiment was repeated with a BF_3 proportional counter embedded in paraffin. For the two measurements, the detector location and the integrated beam current for each proton energy, were kept identical. The sharply peaked distributions, illustrated in Fig. 2, resulting from the mea-

measurements on a thin target, are similar with the two detectors and allow the same accuracy on the extrapolated threshold. The decrease of the yield curve after the first maximum, which is more pronounced with the $[\text{Ge(Li)} + {}^{10}\text{B}]$ detector than with the BF_3 counter, can be related to the smaller solid angle subtended by the ${}^{10}\text{B}$ container, reducing the counting rate above threshold. Furthermore the response of the BF_3 counter with its hydrogenous moderator is almost flat whereas the cross section of reaction in ${}^{10}\text{B}$ decreases continuously with increasing neutron energy.

It should be noted that the 478 keV peak is observed in the spectra taken below the neutron threshold, the Ge(Li) counter being sensitive to the radiations resulting from the $(p, p'\gamma)$ reaction on the Li target. However the shape of the 478 keV line $[\tau = 105 \pm 5 \text{ fs } (10)]$ is different according to the originating reaction: $(p, p'\gamma)$ or $(p, n) + (n, \alpha)$. In the case of the ${}^{10}\text{B}(n, \alpha){}^7\text{Li}^*$ process, the Q value (2.78 MeV) involves a large maximum velocity for the recoiling ${}^7\text{Li}$ ion ($v_0/c = 1.61 \times 10^{-2}$) and consequently the calculated full Doppler broadening in conditions of observation will be equal to 15.4 keV. The variation of the shape of the 478 keV γ peak, for different proton energies near the (p, n) threshold is illustrated in Fig. 3.

We have reported in Fig. 4, the same region in three spectra taken with the $[\text{Ge(Li)} + {}^{10}\text{B}]$ counter for incident proton energies equal to 1890 keV, 2350 keV and 2450 keV, the neutron energy values being respectively equal to 40, 625 and 730 keV. The dominant peak in these spectra corresponds to 478 keV while, as the neutron energy increases, lines arise from inelastic neutron scattering to low excited states of the germanium isotopes given on the label. The 691 keV line, associated with ${}^{72}\text{Ge} (0^+ \rightarrow 0^+)$ internal conversion electrons, has been discussed by different authors (11-13)

and its observation has been proposed for fast neutron flux measurements (13). The adjunction of the ^{10}B element gives in that case an additional sensitivity for slow neutrons which is not available with the usual lithium drifted germanium detector. Furthermore, the isomeric nature of the 691 keV 0^+ state in ^{72}Ge does not make possible submicrosecond timing while the detection of the 478 keV line corresponding to a nuclear level with a short lifetime allows fast timing performances for the counter.



The [$\text{Ge}(\text{Li}) + ^{10}\text{B}$] detector was used to measure the excitation function of the $^{48}\text{Ca}(p, n)^{48}\text{Sc}$ reaction between 1.875 and 2.040 MeV. The detector was located at zero degree to the proton beam, 6 cm behind the target which was prepared by evaporating in vacuo CaCO_3 enriched to 96.8 % in mass 48 onto gold backing. Thickness used was about $15 \mu\text{g}/\text{cm}^2$. Each point corresponds to a beam charge of 2 mC deposited on the target. Areas under the prominent peaks of the spectra were determined at the end of each measurement by the use of an on-line computer. The yields of the 370 keV, 520 keV and 780 keV γ -rays corresponding to transitions in ^{48}Sc and of the 478 keV radiation, resulting from neutron detection, are reported in Fig. 5. A typical gamma-ray spectrum taken at $E_p = 1976$ keV is shown in Fig. 6.

The region of the split analogue of the ^{49}Ca ground state, located around $E_p = 1975$ keV, appears clearly on the yield curves related to γ emission as well as on the neutron emission rate recorded by use of the 478 keV transition. We observe the striking similitude between the 780 keV and the neutron excitation functions. Our results can be compared with those

given by VINGIANI et al (14). In particular, these authors have reported that the components of the split analogue level i. e., the resonances at 1964, 1975, 1982 and 1991 keV have similar decay modes and that the main neutron branch feeds the level at 1402 keV in ^{48}Sc with a relative intensity comprised between 60 and 88 %. This selective decay of the ^{49}Sc analogue resonance ($J = 3/2^-$) into the 1402 keV ($J = 2^-$) level of ^{48}Sc is clearly observed by the use of the [Ge(Li) + ^{10}B] detector.

IV. CONCLUSION

The insertion of boron-10 in the central part of a germanium lithium coaxial counter does not affect the γ detection properties of the device. It allows to improve the performances of previously described neutron detection techniques based upon the $^{10}\text{B}(n, \alpha)^7\text{Li}^*$ reaction taking advantage of the large solid angle and the good resolution for γ -rays. A gamma detector, with in addition a high sensitivity for slow neutrons and from which fast timing signals can be derived, is useful in many different experiments as $(p, n\gamma)$ reactions or delayed neutron studies.

REFERENCES

- 1) C.O. Muehlhause, in *Fast Neutron Physics I*, eds. J.B. Marion and J.L. Fowler, Interscience, New York (1960) 387.
- 2) E.R. Rae and E.M. Bowey, *Proc. Phys. Soc.* 66A (1953) 1073.
- 3) J.H. Neller and W.M. Good, in *Fast Neutron Physics I*, eds. J.B. Marion and J.L. Fowler, Interscience, New York (1960) 570.
- 4) M.S. Coates, G.J. Hunt, C.A. Uttley and E.R. Rae, *Nuclear Data for Reactors*, Conf. Proc. Helsinki (1970) CN-26/35.
- 5) J. Laune, *Neutron Dosimetry II*, eds. Int. Atom. Energy Agency, Vienna (1973) 421.
- 6) R. Bayer, *Nucl. Instr. Meth.* 99 (1972) 339.
- 7) K.H. Beckurts and K. Wirtz, *Neutron Physics*, Springer Verlag, Berlin (1964).
- 8) E. G. Bilpuch, L. W. Weston and H. W. Newson, *Ann. Phys.* 10 (1960) 455.
- 9) *Neutron Cross Sections*, BNL 325 (1964).
- 10) F. Ajzenberg-Selove and T. Lauritsen, *Nucl. Phys.* A227 (1974) 1.
- 11) C. Chasman, K. W. Jones and R. A. Ristinen, *Nucl. Instr. Meth.* 37 (1965) 1.
- 12) P. H. Stelson, J. K. Dickens, S. Raman and R. C. Trammel, *Nucl. Instr. Meth.* 98 (1972) 421.
- 13) D. L. Smith, *Nucl. Instr. Meth.* 102 (1972) 193.
- 14) G. B. Vingiani, R. A. Ricci, R. Giacomich and G. Polani, *Il Nuovo Cimento L VII B* (1968) 453.
- 15) J. B. Marion, F. C. Young, *Nuclear Reaction Analysis*, North-Holland, Amsterdam (1968).

FIGURE CAPTIONS

- Fig. 1 A schematic cross section of the germanium-lithium counter with boron in the central hole.
- Fig. 2 Measurement of the threshold of the ${}^7\text{Li}(p,n){}^7\text{Be}$ reaction using a BF_3 counter or the $[\text{Ge}(\text{Li}) + {}^{10}\text{B}]$ detector.
- Fig. 3 Variation of the 478 keV γ -peak shape, for different proton energies near the threshold of the ${}^7\text{Li}(p,n){}^7\text{Be}$ reaction. Recoil effects in ${}^7\text{Li}(p,p'){}^7\text{Li}$ and ${}^{10}\text{B}(n,\alpha){}^7\text{Li}$ reactions are illustrated by the variation of the width with increasing incident energy.
- Fig. 4 Pulse height spectrum obtained from bombardment of the detector at $E_n = 40, 625$ and 730 keV corresponding respectively to incident proton energies equal to 1890, 2350 and 2450 keV on the lithium target. Lines arise from inelastic neutron scattering to a low excited state of the element given or from ${}^{10}\text{B}(n,\alpha){}^7\text{Li}$ reaction in the boron included in the counter.
- Fig. 5 370, 520 and 780 keV gamma-ray yields from the proton bombardment of a thin ${}^{48}\text{Ca}$ target and measured with the $[\text{Ge}(\text{Li}) + {}^{10}\text{B}]$ counter. 478 keV gamma-ray yield results from neutron detection in the counter and was registered simultaneously.
- Fig. 6 Pulse height spectrum of the γ -rays from the ${}^{48}\text{Ca}(p,n){}^{48}\text{Sc}$ reaction measured at a bombarding energy of 1976 keV. The γ -rays labelled only by energy in keV have been assigned to ${}^{48}\text{Sc}$. The peak labelled 478 keV corresponds to neutron detection in the $[\text{Ge}(\text{Li}) + {}^{10}\text{B}]$ counter.

Table 1

E_n (keV)	$\sigma(n, \alpha)$ (barns)	Absorbed fraction (%)		Overall efficiency*	
		(1)	(2)	(1)	(2)
3	11	70	99	0.28	0.39
10	6	48	90	0.19	0.36
30	3.5	32	75	0.13	0.30
100	1.9	19	52	0.07	0.20
250	0.77	8	26	0.03	0.10

*calculated from the neutron interacting fraction and γ -absorption coefficients for germanium (15) in the used geometry

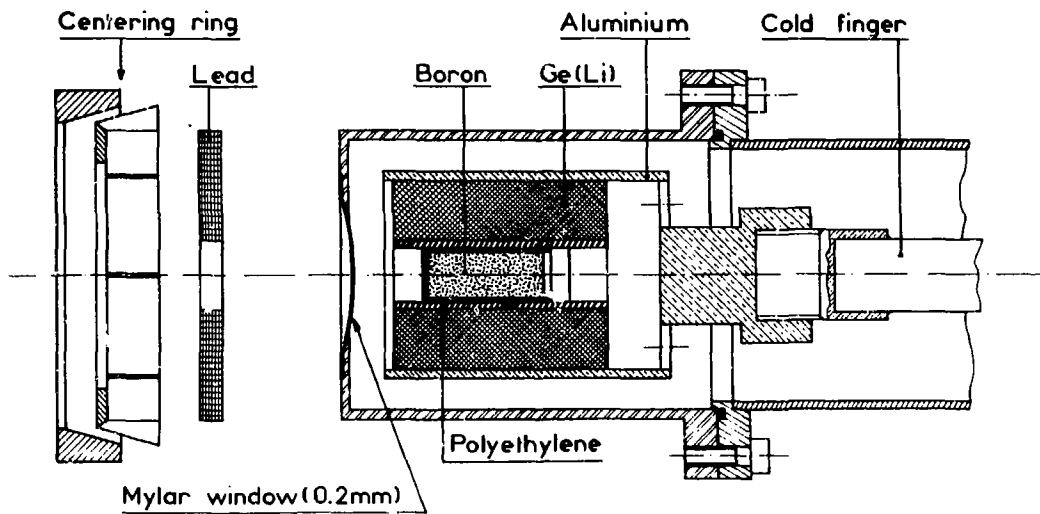


Fig. 1

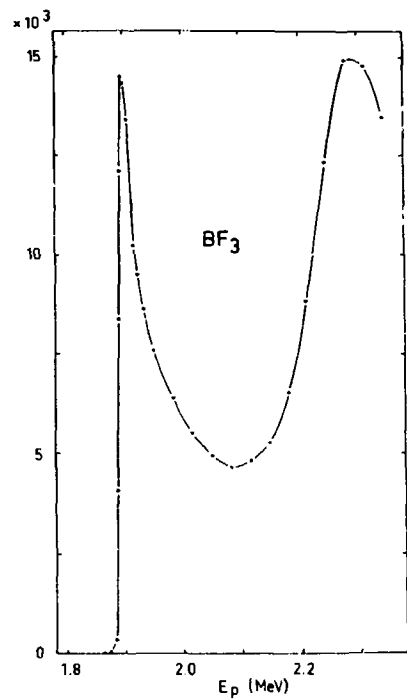
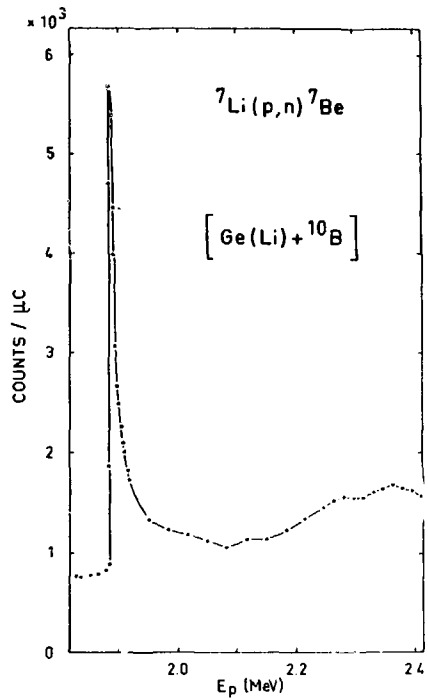


Fig. 2

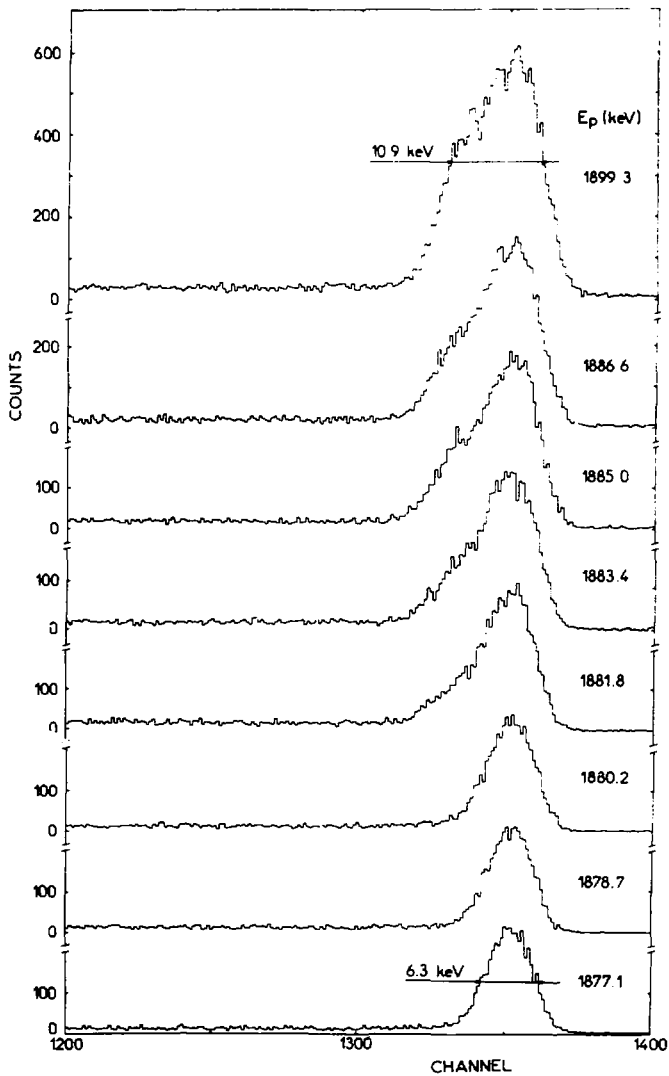


Fig. 3

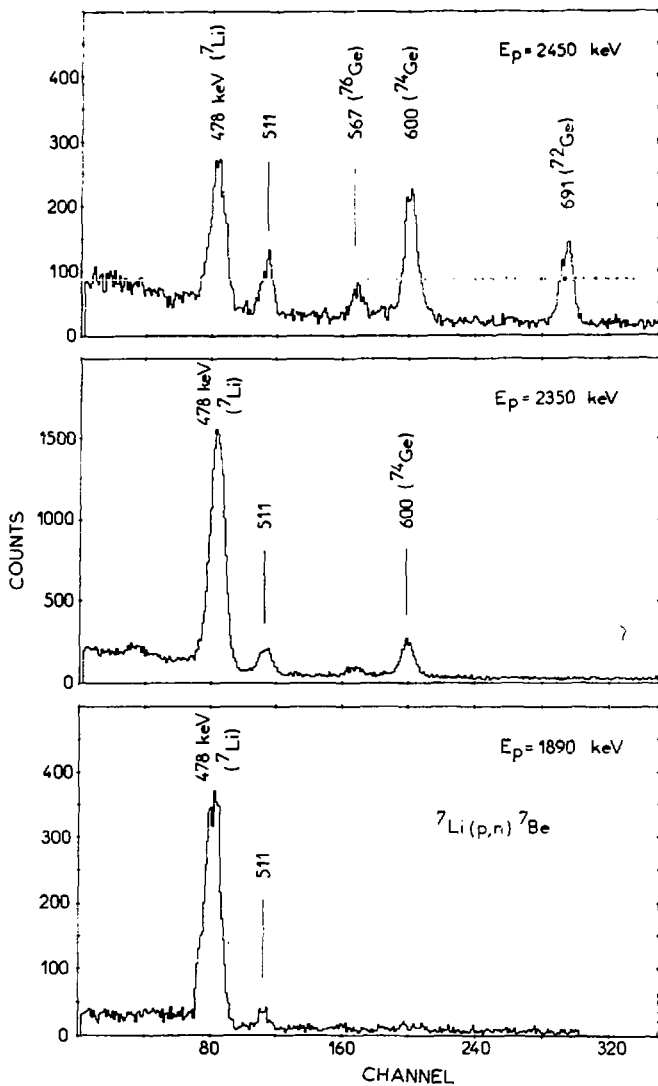


Fig. 4

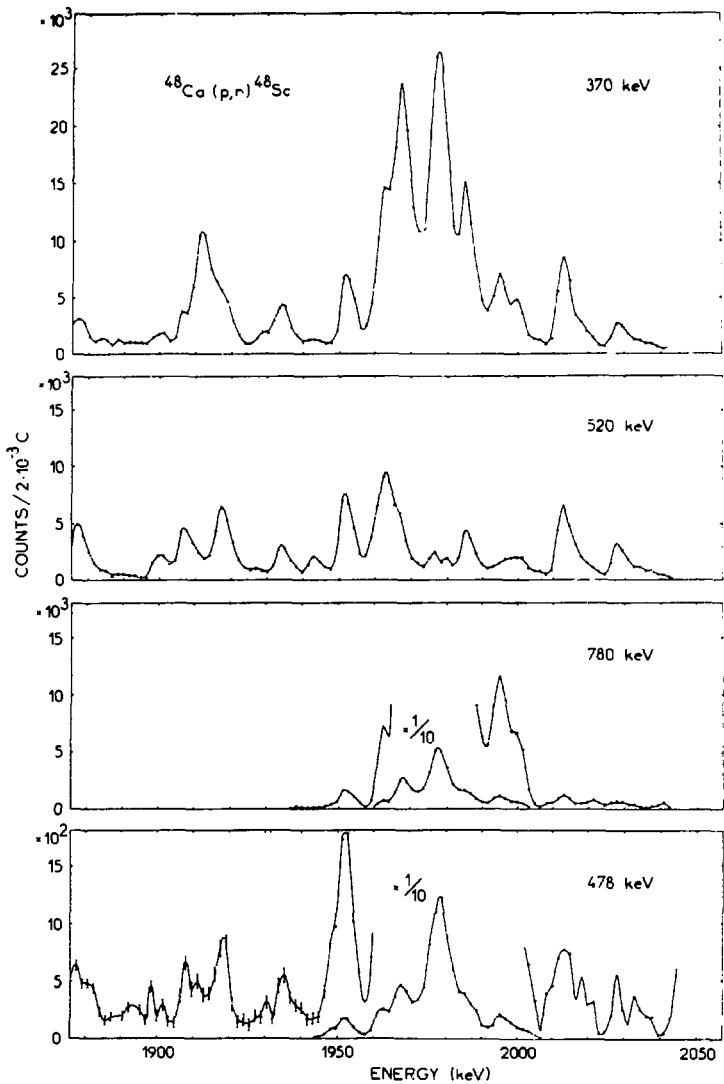


Fig. 5

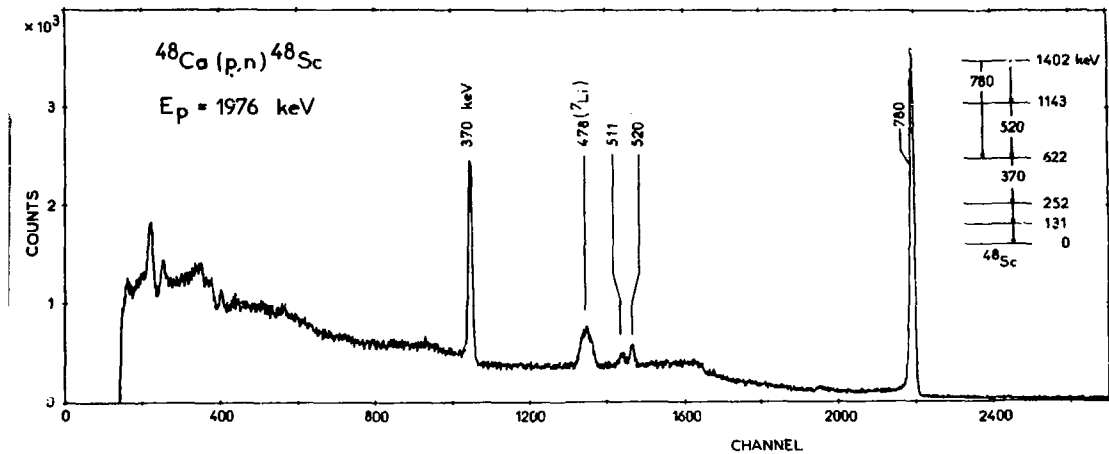


Fig. 6